

Microencapsulation of *Citrus Hystrix* Essential Oil by Gelatin B/Chitosan Complex Coacervation Technique

Siti Afiqah 'Aisyah Murtadza¹, Nurul Asyikin Md Zaki^{1*}, Junaidah Jai¹, Fazlena Hamzah¹, Nur Suhanawati Ashaari², Dewi Selvia Fardhyanti³, Megawati³ and Nadya Alfa Cahaya Imani³

¹*School of Chemical Engineering, College of Engineering, Universiti Teknologi MARA, 40450 Shah Alam, Selangor, Malaysia*

²*Malaysia Genome and Vaccine Institute, National Institutes of Biotechnology Malaysia, Jalan Bangi, 43000 Kajang, Selangor, Malaysia*

³*Department of Chemical Engineering, Faculty of Engineering, Universitas Negeri Semarang, Gunungpati, 50229, Semarang, Indonesia*

ABSTRACT

Complex coacervation is an encapsulation technique used to preserve the bio functionality of essential oils as well as provide controlled release. In this present work, encapsulation of *Citrus Hystrix* essential oil (CHEO) was formed by a complex coacervation technique with Gelatin-B (Gel B) and Chitosan (Chi) as the capping materials. The suitable encapsulation formulation was investigated as a function of pH and wall ratio using Zeta Potential analysis. Turbidity measurement and coacervate yield were carried out to confirm the suitable condition. Total Phenolic Content (TPC) was used to obtain the encapsulation efficiency (EE%) of the process. Results show that the suitable condition for coacervate

formation between Gel B and Chi ratio of 5:1 was at pH 5.8, which produced a high encapsulation efficiency of $94.81\% \pm 2.60$. FTIR analysis validates the formation of coacervate as well as the encapsulated CHEO. The encapsulates obtained were spherical and dominated by 194.557 μm particles. The CHEO was successfully encapsulated by a complex coacervation method.

Keywords: Chitosan, coacervation, encapsulation efficiency, essential oils, gelatin, microencapsulation

ARTICLE INFO

Article history:

Received: 18 February 2023

Accepted: 12 October 2023

Published: 14 March 2024

DOI: <https://doi.org/10.47836/pjst.32.2.07>

E-mail addresses:

aisyahmurtadza@gmail.com (Siti Afiqah 'Aisyah Murtadza)

asyikin6760@uitm.edu.my (Nurul Asyikin Md Zaki)

junejai@uitm.edu.my (Junaidah Jai)

fazlena@uitm.edu.my (Fazlena Hamzah)

suhana_bio@yahoo.com (Nur Suhanawati Ashaari)

dewiselvia@mail.unnes.ac.id (Dewi Selvia Fardhyanti)

megawati@mail.unnes.ac.id (Megawati)

nadya.alfa@mail.unnes.ac.id (Nadya Alfa Cahaya Imani)

* Corresponding author

INTRODUCTION

Citrus Hystrix essential oil (CHEO) has been extensively studied for its beneficial attributes as an antimicrobial (e.g., Sreepian et al., 2019; Srifuengfung et al., 2020) and antioxidant (Venkatachalam, 2019; Wijaya et al., 2017). However, like many other essential oils, its potential application is often limited by its high susceptibility to harsh and extreme environmental conditions (Adamiec et al., 2012). Therefore, encapsulation is a promising technique introduced to improve the stability of essential oils as well as provide controlled release. Encapsulation is a process where essential oils are polymeric coated within a capsule. Adamiec et al. (2012) previously encapsulated CHEO using konjac glucomannan and gum Arabic and reported the efficacy of the encapsulated CHEO in acting as an antibacterial comparable to the standard antibiotics.

Though many techniques could be employed to encapsulate, complex coacervation has been amongst the oldest and most widely used techniques to encapsulate as it offers advantages such as cost saving, simple processes and allows for industrial scalability with very high payloads up to 99% (Bakry et al., 2016; Timilsena et al., 2019). The complex coacervation technique makes use of the principle of separating a colloidal system into two phases: (1) the polymer-rich dense phase (coacervate) and (2) the poor polymer continuous phase (coacervation medium) (Yan & Zhang, 2014). Coacervation formation is induced by the interaction of two oppositely charged polymers, usually using a combination of protein and polysaccharides (Lakkis, 2016). This results in the deposition of wall materials around the core material. The gelatin-gum acacia system is a widely studied and understood coating system (Poshadri & Aparna, 2010). However, there is a need to explore other potential gelatin/polymer systems to further enhance the potential use of encapsulation systems using gelatin. The Latin-chitosan system has been considered a potential combination of polymeric systems encapsulating bioactive compounds. Their combinations have been well-studied for many applications. For example, in a recent study by Wang et al. (2023), their combination was used to stabilize lutein as printable edible inks for food application.

Gelatin is a protein containing many glycine, proline and 4-hydroxyproline residues (Fang & Bhandari, 2010). It can form complex coacervates with large amounts of anionic polymers for its excellent solubility, emulsifying activity, and gelling capability, making it the most commonly used protein for complex coacervation (Wang et al., 2018). Besides that, gelatin is cheap, readily available and possesses relatively low antigenicity compared to collagen. There are two types of commercialized gelatin: Type A gelatin and Type B gelatin, differentiated from its origin (Elzoghby, 2013).

Chitosan is a deacetylated chitin derivative and the second most widely used polysaccharide after cellulose (Vishwakarma et al., 2016). Polysaccharides have been of interest as encapsulating wall material since they can easily be abundant from many sources

(such as algal, microorganisms, plants, and animals) and are low-cost in processing (Yang et al., 2015). It is made up of β - (1 \rightarrow 4) linked monosaccharide units of β -(1,4)-2- amino-2-deoxy-D-glucose. The positive charge of Chi is attributed to the free amino groups that allow for reaction with negatively charged surfaces and anionic polymers (Pedro et al., 2009). Parameters such as the degree of deacetylation (DD) and the molecular weight (MW) of Chi are very important as they could affect the functionality of the polymer (Pedro et al., 2009).

In order to design an optimized coacervation process, an understanding of the physicochemical factors involved in the coacervate formation is crucial. Although many kinds of literature have reported on the optimization of many polymeric systems to achieve a stable coacervate formation (e.g., Ghadermazi et al., 2019; Otálora et al., 2019; Timilsena et al., 2016), the different polymeric system exhibits distinct characteristics, thus, require different optimal parameters to induce coacervate formation. Though previous studies (e.g., Singh & Sheikh, 2022; Fan et al., 2023) have succeeded in encapsulating essential oils using gelatin and chitosan complexes, to our knowledge, no study has been reported on its application to encapsulate CHEO. Therefore, this study used gelatine type B (Gel-B) and chitosan (Chi) as wall materials to encapsulate CHEO through a complex coacervation technique. Since critical factors such as pH and mixing ratio have a great influence on the coacervate formation, the suitable condition was investigated through zeta potential, coacervate yield, and turbidity study. The combination of Gel-B and Chi as wall material should be able to improve the stability of CHEO as well as provide a controlled release to enhance its applications.

METHODOLOGY

Materials

Citrus Hystrix essential oil (CHEO) (pure essential oil) was purchased from BF1 (Malaysia). Gelatin-B (Gel-B) (type B, from bovine) was supplied from Halagel Sdn. Bhd. (Malaysia). Chitosan (Chi) (>80% deacetylation degree) was obtained from Nacalai Tesque (Japan). Oligomeric proanthocyanidins (OPCs), as a naturally occurring source of cross-linker, were derived from the outer shells of red grape seeds; also known as grape seed extracts (GSE-OPCs), contain approximately 98% of proanthocyanidin and was purchased from VitaHealth. Other chemicals used in this experiment were of analytical research grade. Sodium hydroxide (NaOH), Folin & Ciocalteu's Phenol Reagent (FC), and phosphate buffer pH 7 were purchased from R&M Chemicals. As for glacial acetic acid (CH₃COOH), sodium carbonate and ethanol (95%, denatured) were obtained from Friendemann Schmidt, Bendosen, and System Chemicals, respectively. Deionized water (DI) was used throughout the experiment.

Preparation of Stock Solutions

The preparation method of stock biopolymers was adapted from Aziz et al. (2016) with slight modifications. Both biopolymers were prepared at a concentration of 1% (w/v). An adequate amount of powdered Gel-B was first soaked in DI water for 30 minutes. The bloomed Gel-B solution was sealed and left stirring at 300 rpm with a temperature of 50°C for 1 hour. Chi flakes were weighted and dissolved in 1% (v/v) CH₃COOH to prepare Chi solution. The Chi mixture was left stirring (500 rpm) at room temperature for at least 6 hours. Both biopolymer solutions were sonicated for 6 minutes to eliminate the gas bubbles (Dima et al., 2016).

Zeta Potential of Individual Solution

Zeta potential values of the biopolymer solutions were determined using Zetasizer Nano Series (Malvern Instruments Ltd., Worcestershire, UK). Measurements were performed at pH values of 4, 4.4, 4.8, 5.0, 5.2, 5.4, 5.6, 5.8, and 6, as suggested by previous studies (Aziz et al., 2016; Prata & Grosso, 2015). The pH values were adjusted using an aqueous solution of NaOH (0.1 M) and CH₃COOH (0.1 M). Dilution effects from pH adjustment were considered negligible. All measurements were performed in triplicate samples. Results were presented in millivolts (mV) units. A summary of the preparation process is illustrated in Figure 1.

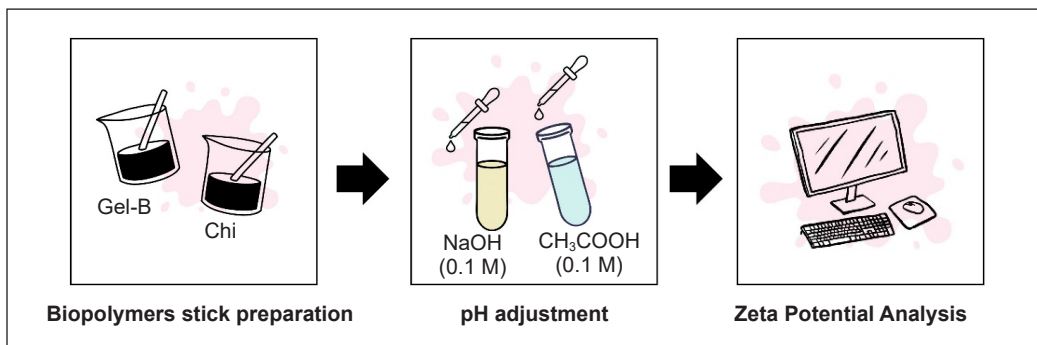


Figure 1. Illustration of the zeta potential measurement process flow

Fourier Transform Infra-Red (FTIR)

In liquid form, FTIR spectra of Gel-B, Chi, and Gel-B/Chi coacervate (pH of 5.8) were obtained using a spectrophotometer FT-IR (Perkin Elmer Inc., Waltham, MA). FTIR spectra were recorded in transmittance (T) mode between 4000–515 cm⁻¹ in the wavelength range.

Preparation of Biopolymers Mixture

Based on the zeta potential result, a mixture of biopolymers was prepared according to the determined ratio of 5:1 between Gel-B and Chi. The total biopolymer volume and concentration were fixed at 60 ml and 1% (w/v) to achieve optimum biopolymer ratios

(Gharanjig et al., 2020). The mixture was stirred for 20 mins at 300 rpm and a temperature of 50°C. Once a homogenized solution was obtained, 10 ml of the mixture was transferred into separate beakers. Then, the pH of the mixture was adjusted using an aqueous solution of NaOH (0.1 M) and CH₃COOH (0.1 M) to obtain desired pH of 5.0, 5.2, 5.4, 5.6, 5.8 and 6. To ensure the biopolymers ratio was maintained, a different sample of the mixture was used for each pH value.

Dilution effects from pH adjustment were considered negligible. When the desired pH was obtained, the sample mixture was left stirring at 300 rpm and 50°C for 15 minutes to ensure the homogeneity of the solution. The best operating pH was selected for maximum coacervate formation using coacervate yield and turbidity analysis. For turbidity analysis, turbidity measurement was taken on each sample using UV-Vis (Agilent Technologies Cary 60 UV-Vis) at 600 nm (Kang et al., 2012). Distilled water was used as blank. Results were presented in absorbance value. The sample was centrifuged at 3000 rpm for 30 minutes to determine coacervate yield. The supernatant was decanted, and the sediment was left dried in an oven from 50°C to 60°C until the constant weight of the dry coacervate was achieved. A summary of the preparation process is illustrated in Figure 2. Coacervate yield (CY%) refers to the percentage of coacervate weight versus the total weight of biopolymers used to prepare the coacervate and was calculated as Equation 1:

$$CY\% = \frac{W_c}{W_{all}} \times 100\% \quad (1)$$

where W_c is the weight (g) of dry coacervate, and W_{all} is the weight (g) of the total biopolymers used to prepare the coacervate.

All measurements were performed in triplicate samples. FTIR, zeta potential analysis and visual evaluation were performed on each sample as described previously to better understand the coacervate formation.

Encapsulation of CHEO

The overall process of encapsulating CHEO was carried out using the adapted method from Aziz et al. (2016) and Rungwasantisuk and Raibhu (2020). Before encapsulation, a stock of biopolymers was prepared as previously described. The encapsulation procedure was divided into eight steps. All necessary information, including sample preparation, equipment settings, and operating parameters, were summarized in Figure 3.

Morphology Analysis of Encapsulates

The morphology of encapsulates in the suspension was revealed using an optical microscope (RZ-5, Meiji Techno, Japan) alongside a digital camera and registered under Image Pro Plus 4.0 software. The microscopic images were taken at 40× magnification.

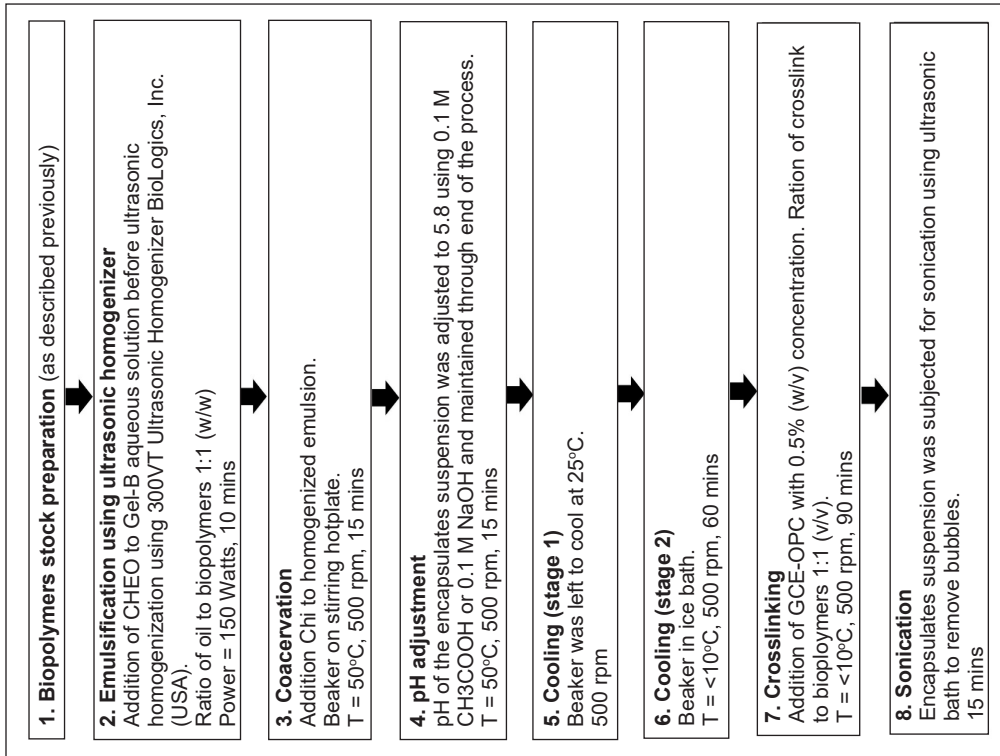


Figure 3. Procedure to encapsulate CHEO using Gel-B and Chi

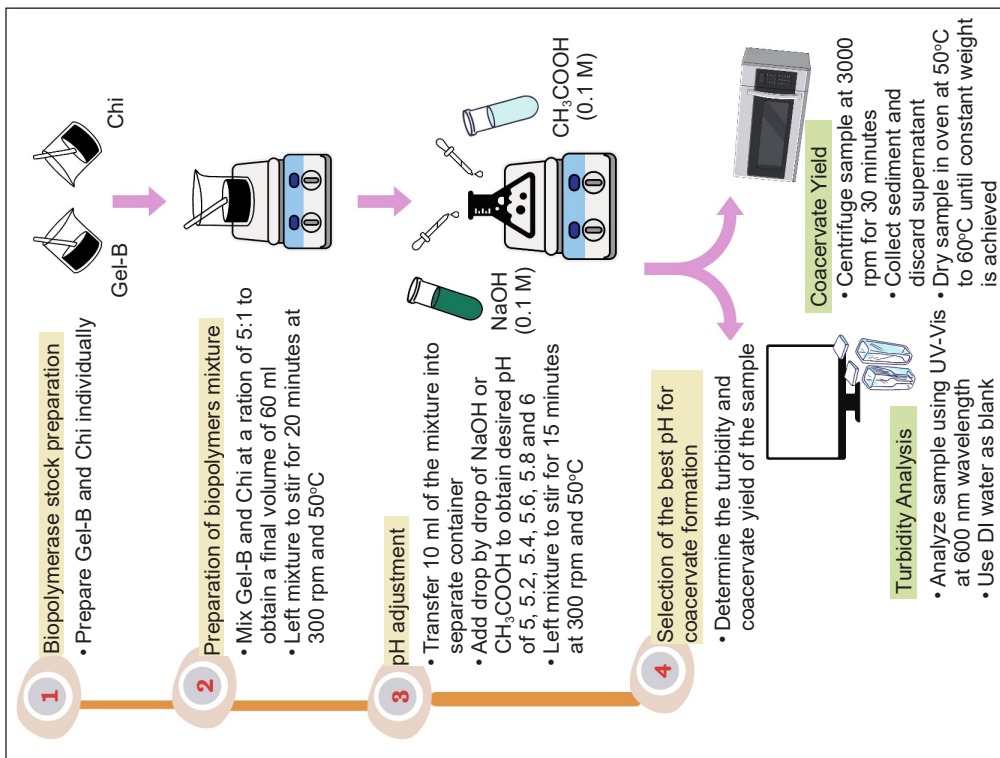


Figure 2. Illustration of the preparation of biopolymers mixture

Particle Size Analysis

Determination of the encapsulate size in the suspension and particle size distribution were conducted using laser light scattering (Mastersizer 2000, Malvern Instruments Ltd., Worcestershire, UK) at 1 min, 2500 rpm. An appropriate portion of the wet encapsulates was added dropwise to the instrument's wet dispersing accessory. Triplicate samples were analyzed, and the mean volumetric diameter (D_{4,3}) was reported.

GCMS

Gas Chromatography–Mass Spectrometry (GCMS) analysis was conducted to identify the phenolic compounds and terpenoids present in the CHEO. The analysis was performed using an Agilent 7890 gas chromatograph model coupled to an Agilent 5975 quadrupole mass detector (Agilent Technologies, Santa Clara, CA, USA). The operating method was adopted by Ashaari et al. (2021). One microliter of CHEO was injected into the GC injection port with a 1:50 split mode and separated on an HP-5MS capillary column (30 m × 250 µm inner diameter × 0.25 µm film thickness). Helium was used as carrier gas with a flow rate set at 1 mL/min. The operation temperature was programmed at a rate of 10°C/min to increase the temperature gradually from 50°C to 280°C in 3 minutes. The electron-impact (EI) mode was used while operating the spectrometer with 70 eV ionization energy. The inlet/transfer line and ionization source temperatures were set at 280°C and 220°C, respectively. The volatile components of CHEO were identified through mass spectra comparison using MSD Chemstation Enhanced Data Analysis Software (E.02.02.1431 version, Agilent Technologies) and the National Institute of Standards and Technology library database (NIST 20).

TPC Quantification

Total Phenolic Content (TPC) quantification of CHEO was carried out using the Folin-Ciocalteu method as described by Shetta et al. (2019) and Do et al. (2014) with slight modifications. 1 ml of CHEO (0.9203 g/ml) was added into 9 mL of ethanol and diluted 10x with DI water. Then, 1 mL of previously diluted CHEO mixture was mixed with 2.5 ml of freshly prepared FC reagent diluted in water (10% v/v). The solution was left for 3 minutes incubation at room temperature and in dark conditions. Then, 2.0 ml of Na₂CO₃ (7.5% w/v) was added to the solution and mixed again. After 30 minutes of reaction time at ambient temperature (25°C) and in dark conditions, the absorbance of the sample was measured at 765 nm wavelength against blank using UV-Vis (Agilent Technologies Cary 60 UV-Vis). TPC of CHEO was determined as Gallic Acid Equivalents (GAE) by entering the absorbance value of CHEO extracted to the equation of the Gallic Acid standard curve that was initially prepared ($y=0.12523x + 0.03961$; $R^2=0.99870$). The result was used as a control to calculate the amount of CHEO for encapsulation efficiency. All measurements were performed in triplicate samples.

Determination of Encapsulation Efficiency

This study determined the amount of unencapsulated CHEO by analyzing the excess CHEO available in the suspension after the encapsulation process. 5 ml of accurately measured homogenized encapsulated suspension was placed in a 15 ml tube. Then, 30 mL of ethanol was added into the tube to extract unencapsulated oil. The solution was then mixed up using a vortex mixture for 5 minutes at 1500 rpm (Fraj et al., 2021; Yu et al., 2017) to enhance the extraction of unencapsulated oil. After extraction, the dispersion was filtered using a Whatman #41 paper filter (Shi et al., 2018). The free (unencapsulated) oil filtrate was collected and evaluated for spectrophotometric quantification of total phenolic compounds using UV-Vis (Agilent Technologies Cary 60 UV-Vis) at 765 nm wavelength. All measurements were performed in triplicate samples. The encapsulation process efficiency (EE%) was calculated as Equation 2 (Girardi et al., 2017):

$$EE\% = \frac{W_0 - W_s}{W_0} \times 100\% \quad (2)$$

where EE% is the weight percentage of encapsulated CHEO in a certain amount of encapsulated suspension, W_s is the weight (g) of unencapsulated CHEO in a certain amount of encapsulated suspension, and W_0 is the weight (g) of the CHEO used to prepare the same amount of encapsulates suspension.

Statistical Analysis

All experiments were carried out at least three times under the same conditions. Results were presented as average with standard deviation values. Statistical analysis was performed using Microsoft Excel and IBM SPSS software. Determination of the statistical difference between groups and probability value of $p < 0.05$ was specified with a one-way analysis of variance (ANOVA) using Post hoc Tukey's test.

RESULTS AND DISCUSSION

Analysis of Individual Biopolymer

Recently, determining the zeta potential of individual polymers has become an interest since it could help to reduce the number of assays needed to determine the pH range where interaction between polyelectrolytes possible to occur (e.g., Espinosa-Andrews et al., 2013; Gharanjig et al., 2020). Protein and polysaccharides usually carry a functional group that gives them either a positive or negative charge depending on the introduced pH.

Figure 4 presents the zeta potential of individual Gel-B and Chi at different pHs from 4.0 to 6.0. As can be observed from the Figure 4, all zeta potential values over the pH range tested for Chi are positive. It indicates that Chi is positively charged and could

function as a polycation in the pH range between 4.0 and 6.0. Chi naturally exhibits cationic properties in an acidic environment due to the protonation of amino groups, thus making it soluble in water (Aziz et al., 2016; Cheung et al., 2015). However, the zeta potential values are decreasing as the pH approaches 6.0. According to Espinosa-Andrews et al. (2013), this decreasing behavior occurred due to the loss of charge of the glucosamine segments and the reduction of any electrostatic screening effects. For Chi to become soluble in an aqueous form, the pH of the solution must be less than its pKa (6.5) (Prata & Grosso, 2015), or otherwise, it will become insoluble, precipitates (Sogias et al., 2010) and manifests in the formation of a cloudy solution. Preliminary studies in this experiment have shown that at pH 6, the solution turns cloudy, and therefore, considering the solubility of Chi, the pH selected is limited to only 6 (Gonçalves et al., 2018).

On the other hand, the zeta potential values for Gel-B show positive values between pH 4 and 5 and negative values from pH 5.2 up to 6.0. Similar to the findings by Lv et al. (2012), in which Gel-B exhibits amphoteric characteristics. Typically, Gel-B is an anionic protein with an isoelectric point (pI) between pH 4.8–5 (Elzoghby, 2013). From the analysis of the result, we found that the pI of Gel-B was approximately at pH 5.1. At this pH, Gel-B exhibits a zero-charge density from shielding the carboxylic moieties by excess H⁺ counterions (Espinosa-Andrews et al., 2013). In designing operating conditions for complex coacervation, it is important for protein and polysaccharide to have opposite charges to induce coacervate formation from the electrostatic interactions through carboxylate groups located on Gel-B and protonated amine/amide of Chi. Above the pI value, Gel-B will behave as an anionic protein through dissociation of the carboxylic groups ($-\text{COOH} \rightarrow -\text{COO}^- + \text{H}^+$) and, hence, able to neutralize the protonated amine groups of cationic polysaccharides (Chi). Thus, in this study, pH 5.0, 5.2, 5.4, 5.6 and 6.0 were selected for further study.

Determination of the Best pH and Wall Ratio for Complex Coacervates Formation

Optimizing a coacervate formation is a complex process as critical parameters such as pH and mixing ratio need to be individually optimized as they are interdependent (Yan & Zhang, 2014). The mixing ratio is an important factor for optimum coacervate formation as

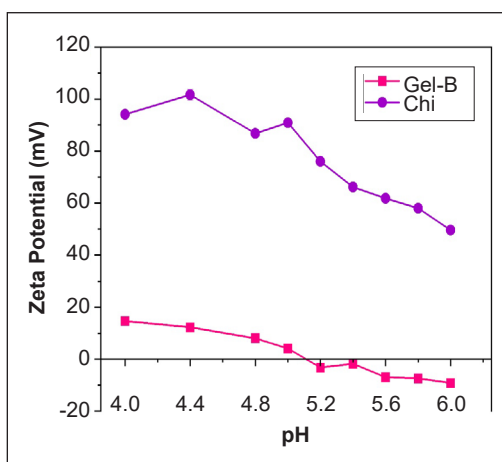


Figure 4. Zeta potential value for Gel (B) and Chitosan

it indicates the charge balance between the protein and polysaccharide involved (Kaushik et al., 2015) and determines the intensity of interaction and complexation (Eghbal & Choudhary, 2018). Timilsena et al. (2016) reported that an optimum coacervation was achieved at a mixing ratio of chia seed protein isolate (CPI) to chia seed gum (CSG) of 6:1 at an identified optimum pH of 2.7. Further increase of CPI in the mixing ratio at the same pH results in decreased coacervate yield. Increasing the ratio from its optimum proportion will cause one component to become deficient and another in excess (Timilsena et al., 2019). The excess polymer will not be able to react with soluble form in the equilibrium phase. Meanwhile, in a study by Gharanjig et al. (2020), the authors found that a decreasing pattern of pH optimum was observed as they increased the ratio of gum to gelatin. It indicates that pH influences coacervate formation, and a specific optimized mixing ratio at different pH exists. An optimum mixing ratio occurs when both polyelectrolytes are in equivalent amounts in which none of the polyelectrolytes are in excess. Therefore, zeta's potential evaluation should exhibit a charge of zero or almost near zero (Emamverdian et al., 2020).

The data from zeta potential values of individual polymers can be used to develop a mixing ratio between Gel-B and Chi (Prata & Grosso, 2015). Theoretically, if an anionic protein has a -5mV charge and a cationic polysaccharide carries a 25mV charge at pH titration of 5. Thus, it would be necessary to increase the use of protein 5 times to neutralize the positive charge of polysaccharides, whereas the mixing ratio for protein to polysaccharides would be 5:1.

Table 1 presents five possible mixing ratios of Gel-B:Chi; 24:1, 7:1, 36:1, 9:1, 8:1 and 5:1 that were developed by taking into account charge on both biopolymers. However, considering economic interest, only a mixing ratio of 5:1 was used for further analysis since this combination ratio used the least amount of biopolymers as the raw materials.

Table 1
Developing wall ratio from Gel (B) and Chi charge

pH	Gel	Chi	Multiplier	Round off	Gel:Chi	
4	14.67 ⁱ ± 0.06	94.15 ^g ± 0.49	-	-	-	-
4.4	12.27 ^h ± 0.23	101.67 ^h ± 2.08	-	-	-	-
4.8	8.03 ^e ± 0.10	86.80 ^f ± 1.06	-	-	-	-
5	4.10 ^f ± 0.04	90.87 ^g ± 1.10	-	-	-	-
5.2	-3.23 ^d ± 0.03	76.03 ^c ± 0.78	-23.56	~24	24	1
5.4	-1.83 ^e ± 0.01	66.17 ^d ± 1.33	-36.16	~36	36	1
5.6	-6.94 ^c ± 0.07	61.83 ^c ± 0.86	-8.91	~9	9	1
5.8	-7.45 ^b ± 0.27	58.00 ^b ± 0.56	-7.78	~8	8	1
6	-9.18 ^a ± 0.11	49.60 ^a ± 1.08	-5.41	~5	5	1

Note. The superscript alphabet denotes the statistically significant difference between groups ($p < 0.05$) for each column. The level of significance is determined by alphabetical order. Groups with the same alphabet indicate no statistical difference between groups.

The interaction between two biopolymers can become evident in several ways: (1) small soluble complexes (SC) are formed by manifesting themselves in murky solutions, and (2) depending on interaction; if the interaction is weak, a homogeneous weak gel is formed, but if the interaction is strong, precipitation of both biopolymers will occur (Espinosa-Andrews et al., 2013). Many literatures (e.g., Kaushik et al., 2015; Lv et al., 2013; Shinde & Nagarsenker, 2009) have reported on different evaluation methods used to validate the formation of this precipitate or coacervate. Common methods include turbidity/visual appearance, coacervate yield, and zeta potential analysis. Turbidity is related to the concentration of the polyelectrolyte solutions and their molecular weight (Meka et al., 2017). The coacervate formation will reduce the transparency of the biopolymer mixture, causing a higher absorbance value (Kang et al., 2012). Meanwhile, the use of zeta potential or electrophoretic mobility to predict the extent of coacervate formation has been explained by Burgess and Carless (1984).

Sometimes, observing more than one method to validate each parameter is compulsory. For instance, one should consider the relationship between the absorbance increase and insolubility in justifying turbidity measurement alone. In some cases, like a study by Prata and Grosso (2015), they found that the turbidity of a system with a pH greater than 6.5 represents the insolubility of the Chi rather than the formation of complexes owing to a large number of reactive groups in Chi. Though significant electrostatic interaction that initiates complex coacervation is induced from the large charges on the polyelectrolytes, charges that are too large will cause precipitation (Aziz et al., 2016).

The coacervate yield and absorbance value of coacervate formation over a range of pH tests are presented in Figure 5. As can be seen from the Figure 5, both dependent variables showed a similar pattern, validating each other responses towards pH variables that were being tested in the experiment. As demonstrated by one-way ANOVA, a statistically significant difference was observed in both dependent variables: coacervate yield ($F(5,12)=61.229, p=0.001$) and absorbance ($F(5,12)=91.865, p=0.001$) illustrating legitimate pH effects towards both dependent variables tested. However, in both dependent variables, a statistically significant difference was more prominent at lower pH ranges as compared to higher pH ranges. This statistical evidence also implied the need to observe at least two validating parameters, as mentioned before, since the coacervate yield and absorbance value were unlikely to be statistically significant toward pH values at higher pH tests.

In particular, the coacervate yield and absorbance values were highest at pH 5.8 compared to other pH ranges, indicating the highest coacervate formation occurred at this pH. Therefore, this pH should be maintained to achieve an optimum coacervate formation for a mixing ratio 5:1 between Gel-B/Chi. A quite similar finding was also reported by Kang et al. (2012) when encapsulating using a combination of Gel-B and Chi. Though the study indicated that the best mixing ratio and pH for Gel-B and Chi are 15:1 (w:w)

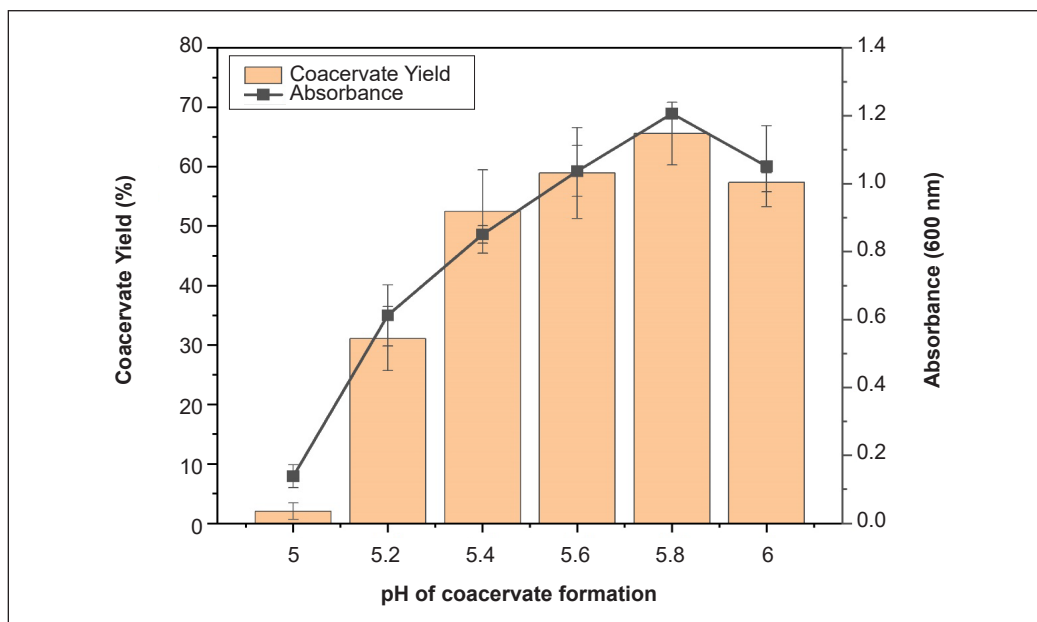


Figure 5. Absorbance value for Gel (B)-Chi (5:1) mixture (Alphabet is used to denote the statistically significant difference between groups ($p < 0.05$). Given coacervate yield: pH 5.0^a, 5.2^b, 5.4^c, 5.6^c, 5.8^c, 6.0^c; absorbance: pH 5.0^a, 5.2^b, 5.4^c, 5.6^{cd}, 5.8^d, 6.0^d. Level of significant is determined by alphabetical order. Groups with the same alphabet indicates no statistical difference between groups)

and 6.0, respectively, the actual ratio between glucosamine residue of Chi and acidic amino acid residue of Gel-B was calculated to be roughly 1:5. Another study reported by Espinosa-Andrews et al., (2013) has shown that a shift towards a higher optimum pH (> 5) was observed when a smaller ratio between Gum Arabic and Chi was used; [5.5:1], [3:1], [1:1], meaning when Chi as polycation was in excess, optimum pH is more likely to be achieved at higher pH value.

It also explained the unlikely statistically significant difference of coacervate formation observed in our study at higher pH values tested. A good justification for this observation is that when the basicity of the system increases, the absolute charge density of Chi decreases but remains in the positive region. At the same time, the zeta potential of Gel-B achieves a maximum degree of ionization, as seen in Figure 4. Therefore, the zeta potentials of Chi and Gel-B become almost equivalent, rendering a complex with almost no/near to zero residue charge. A zero or near-to-zero residue charge of the complex would reduce electrostatic repulsions between particles and colloidal stability of the system, causing precipitates and, hence, resulting in maximum turbidity and coacervate yield.

Meanwhile, Figure 6 shows the behavior of charge density and the visual appearance of the coacervate. Two significant pieces of information should be observed. First, all coacervates exhibit a positive charge density value regardless of pH. The inference derived was an excess of Chi (Prata & Grosso, 2015) as polycations in the system. As observed

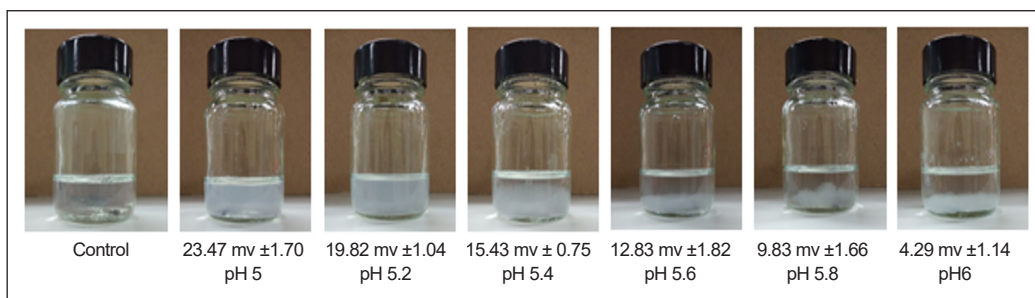


Figure 6. Visual evaluation and zeta potential of Gel (B)-Chi mixture

in Figure 4, Chi exhibits a larger absolute charge density than Gel-B; thus, more Gel-B is needed to neutralize the positive charge of Chi. However, this mixing ratio might not be the ideal for Gel-B and Chi used in this study. Second, the charge density of coacervate showed a decreasing pattern when the pH was increased. As discussed previously, this observation agrees with the absorbance and coacervate yield result. More coacervate was formed when the pH was increased, but at pH 6.0, the reduction observed was contributed by the influence of the alkali addition, which tends to neutralize the negatively charged group of the Chi (Prata & Grosso, 2015). In a study by Silva and Andrade (2009), the author also found a significant reduction in turbidity for all combinations of Gel-B and Chi systems studied at pH 6.0.

As evidence, analysis of individual polymers showed the carboxylate groups located on proteins and protonated amine/amide of the polysaccharides (Gharanjig et al., 2020). The negative charge of proteins is associated with the presence of carboxylate groups. Figure 7 shows the FTIR spectrums related to Gel-B, Chi, and their complex coacervate analyzed at pH 5.8. As shown in Figure 7, the three spectrums showed an overall similar pattern with two significant peaks. A wide, strong peak was observed at wavelength 3308.61 cm^{-1} and 3337.03 cm^{-1} for Gel-B and Chi, respectively. These peaks correspond to normal polymeric O-H stretching vibrations and N-H stretching of amines and amides. Characteristic peaks of Chi were due to the stretching and bending from O-H groups of the pyranose ring and the stretching vibration of N-H functional groups of the primary amine in Chi's backbone (Roy et al., 2018). Meanwhile, short, weak peaks at 1635.24 cm^{-1} for Gel-B and 1636.13 cm^{-1} for Chi result from the N-H bending of amines and the C-O stretching of amides.

The formation of coacervates between Gel-B and Chi was evidenced by a slight change in the coacervate spectrum, suggesting that the functional groups of coacervate underwent substantial alteration. A shift towards a lower wavelength range was due to the formation of hydrogen bonds between Chi and Gel-B molecules. Notably, the resultant coacervate spectrum exhibits slightly lower absorption strength at around 3207.91 cm^{-1} compared to native biopolymers alone due to interaction between the C=O group of Gel-B and the N-H groups of Chi. As stated before, the formation of complex coacervate between Gel-B

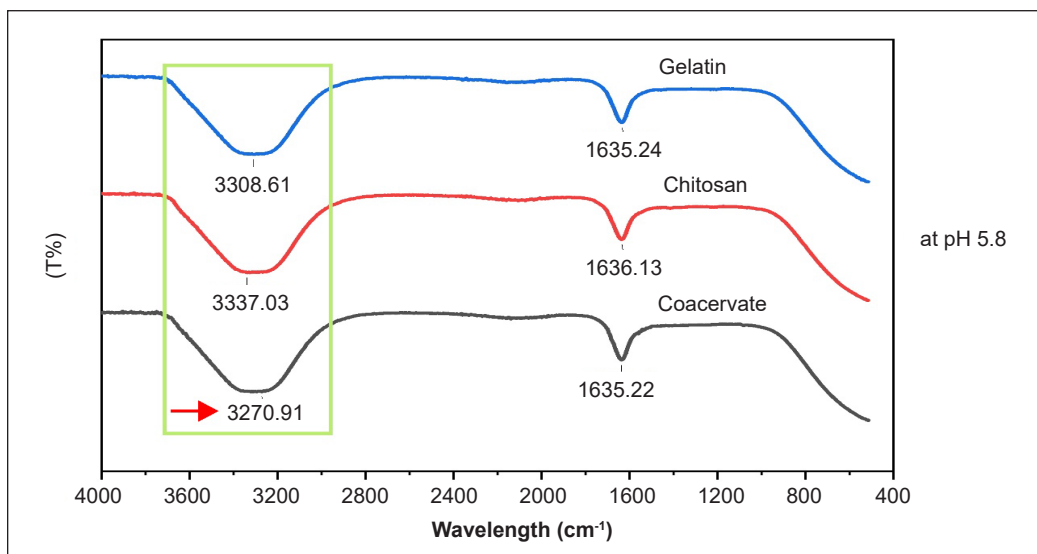


Figure 7. FTIR spectrums related to Gel-B, Chi and their complex coacervate at pH 5.8

and Chi was driven by the electrostatic interactions through carboxylate groups located on Gel-B and protonated amine/amide of Chi.

Characterization of CHEO

Analysis of the TPC in the CHEO used in this study confirmed the presence of CHEO contains almost 2.01 ± 0.02 mg of GAE/g of oil. The TPC value obtained was expected to be lowered compared to findings from Wijaya et al. (2017) and Houg et al. (2023) since CHEO used in this study was simply purchased from available commercialized CHEO. Some susceptible phenolic compounds might have been lost throughout the extraction and manufacturing processes. Deterioration of the compounds or volatile loss is likely to occur owing to the high temperature and long duration of the extraction procedures (Phong et al., 2022). Besides, different amounts and variation types of active constituents found in CHEO are due to various factors such as the method of extraction (Wijaya et al., 2017) and agroclimatic influences such as seasonal, geographical, or climatical of the location where CHEO was obtained (Ahmed et al., 2019).

From the analysis of GCMS data, 102 chemical compounds were identified in CHEO and used in this experiment. Such compounds would include Isopropyl myristate (41.3399%), Isopropyl palmitate (26.5571%), D-Limonene (4.6678%), Polypropylene glycol (4.2105%), Solvanol (3.4694%), Hexylcinnamaldehyde (2.6428%), d-Camphor (2.5863%), Palmitic acid (2.3143%), Myristic acid (1.8121%), Dipropylene glycol (1.4956%) and other compounds that make up less than 1% of the total composition of CHEO (Table 2).

Based on the result, it can be concluded that some of the major compounds typically presented in CHEO (Lubinska-Szczygeł et al., 2018; Othman et al., 2016) that belong to the terpenes were detected such as D-Limonene, linalool, α -Terpinol, L- β -Pinene, L-4-terpineol, d- α -Pinene, Terpinolene, Citronellol, β -mircene, Camphene, Citronellyl palmitoleate, α -Sabinene, β -Copaene and citronellal. The bio functionalities of CHEO as an antimicrobial and antioxidant are mainly contributed by the synergistic effects between these active constituents present in CHEO (Qin et al., 2018). Ensuring these active constituents are successfully entrapped should be a primary concern when encapsulating CHEO.

Table 2
List of chemical constituents present in CHEO

RT	Compound	%
15.9973	Isopropyl myristate	41.3399
17.9849	Isopropyl palmitate	26.5571
5.7856	D-Limonene	4.6678
6.6560	Polypropylene glycol	4.2105
13.6688	Solvanol	3.4694
15.3067	Hexylcinnamaldehyde	2.6428
7.5516	d-Camphor	2.5863
18.0257	Palmitic acid	2.3143
16.1052	Myristic acid	1.8121
5.9371	Dipropylene glycol	1.4956

Encapsulation Efficiency

One of the important parameters to evaluate the performance of an encapsulation process is calculating the encapsulation efficiency (EE) value. Encapsulation efficiency (EE) is the percentage of essential oil successfully entrapped within the wall material over the essential oil introduced at the beginning of the process (De Matos et al., 2018). Previous studies (e.g., Hussein et al., 2016; Rosli et al., 2018) have shown that Total Phenolic Content (TPC) can be used to calculate EE for essential oil encapsulation. This experiment achieved a high EE value at almost $94.81\% \pm 2.60$. This result is expected as, according to Timilsena et al. (2019), complex coacervation provides a high EE value of up to almost 99%. Other studies by Manaf et al. (2018) and Mousavi et al. (2021) also reported high EE values at around 94% and 87% when using Gel-B and Chi as their capping material. A high percentage of encapsulation efficiency indicates that less CHEO is present on the surface of encapsulates or not encapsulated in the process. It also implies that the encapsulation process was conducted successfully, and that Gel-B and Chi can be used as the perfect combination of wall materials to encapsulate CHEO.

Physical Properties of Encapsulates

Generally, the types and structure of encapsulates produced are influenced by the wall materials used and the encapsulation condition and method (Bakry et al., 2016). Different characteristics in terms of morphology and size of encapsulates can be obtained by manipulating chemical, physical, and condition parameters throughout the

encapsulation process (Aziz et al., 2015; Aziz et al., 2014). Figure 8 shows the image of encapsulates under observation using an optical microscope at 40× magnification. It can be seen from the Figure 8 that the encapsulates produced were spherical, mononucleated, and a single core with a definite wall (Fang & Bhandari, 2010), as indicated in the red circles. This finding was also in line with encapsulates produced in a study by Oliveira et al. (2019), who observed encapsulates with mononuclear structures when encapsulating pequin oil with gelatin and gum Arabic using complex coacervation. However, this result was in contrast with the findings from Raksa et al. (2017).

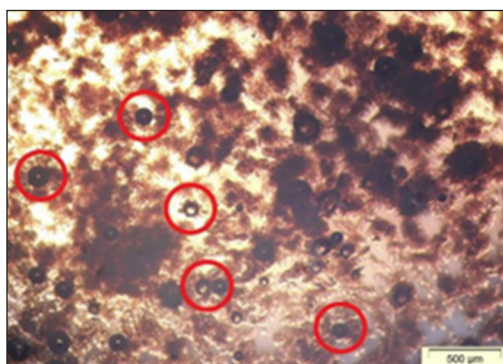


Figure 8. Optical microscopic image of wet encapsulates prior encapsulation process taken at 40× magnification (Red circles indicate individual wet encapsulates produced in the suspension)

In the study, the authors observed encapsulates with spherical and matrix-type structures in which loading of CHEO presented as small spherical particles inside the encapsulate. The formation of a matrix type or multicore encapsulates is caused by the aggregation of many single-core encapsulates and could be seen in encapsulation using the coacervation process (Dong et al., 2007; Wang et al., 2014). Meanwhile, in the encapsulation process, which involves thermal treatment such as spray drying, the formation of a multicore structure might be caused by the outward movement of a small amount of volatilized EOs that are later embedded inside the crust wall (Adamiciec et al., 2012) or stays on the surface (Ngamekaue & Chitprasert, 2019). As found in our study, the formation of mononucleated structure encapsulates could be due to the homogenization step involved during the emulsification process.

Lemetter et al. (2009) investigated the effect of shear rate on the formation of encapsulates and discovered that as the rotation speed increased, more mononucleated encapsulates were detected. It is also interesting to note that most encapsulates in this study were well dispersed as individuals in the suspension with less agglomeration as compared to encapsulates produced by Aziz et al. (2016). The author obtained the final products of encapsulates clustered together, forming agglomerates, and justified that excess Gel-B or the wall materials that underwent phase changes from liquid to solid were likely to go through a sticky stage, making it difficult to avoid agglomeration. Meanwhile, Prata and Grosso (2015) inferred that unencapsulated oil on the encapsulated surface would, over time, promote encapsulates to attach and form agglomerates.

However, less agglomeration observed in our study could be due to less polymer concentration used in the coacervation process than Aziz et al. (2016). While Burgess and

Carless (1985) justified the reduction in coacervate formation was due to the increment in the polymer concentration, Oliveira et al. (2019) used this justification to explain the formation of agglomeration when investigating the effect of concentration on the morphology of encapsulates produced. It is inferred that as the concentration of polymers increases, the neighboring molecules are induced to neutralize each other through coulombic attraction, forming a large, stable gel-type network fortified by hydrogen bonding.

The size distribution of encapsulates is shown in Figure 9. As can be seen, a monomodal distribution was observed in which the largest particle size, $d(0.9)$ of 194.557 μm , was dominating. The encapsulates were also characterized by a mean size diameter $d(4,3)$ of 108.395 μm . The size range is within an acceptable range of microparticles produced from the complex coacervation process, which is between 0.1–500 μm (Comunian & Favaro-Trindade, 2016), suggesting that the encapsulation technique employed in this study successfully produced microencapsulates. The width of distribution (span) was considered small (2.398) owing to the mononucleated structure and homogenization process preventing multicore encapsulation formation through aggregation.

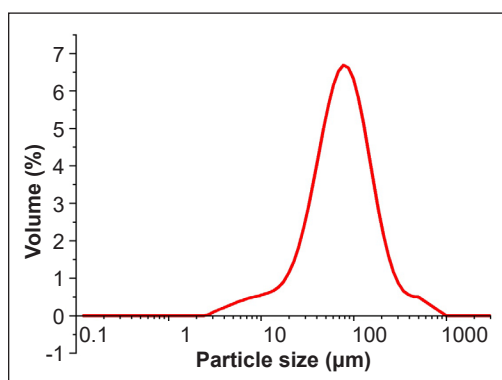


Figure 9. Size distribution of wet encapsulates

CONCLUSION

In the present study, CHEO encapsulates were successfully produced and characterized through complex coacervation. Gel-B and Chi were excellent wall materials to encapsulate CHEO at 5:1 and pH 5.8 mixing ratios. FTIR analysis confirmed the formation of coacervates between Gel-B and Chi. These operating conditions obtained a high EE value at almost $94.81\% \pm 2.60$. Characterization of CHEO used in this study revealed the presence of phenolic compounds at 2.01 ± 0.02 mg of GAE/g of oil. From GCMS data analysis, major compounds presented in the CHEO belong to the terpenes group. The encapsulates produced were spherical with a mononucleated structure and had a particle size within the microcapsule range between 23.270 μm and 194.557 μm .

ACKNOWLEDGEMENTS

This work was funded by Malaysia's Ministry of Education (MOE) Fundamental Research Grant Scheme (FRGS) through a 600-RMI/FRGS/5/3 (186/2019) grant. We are very grateful for the assistance provided by all parties in assisting the research activities.

REFERENCES

- Adamiec, J., Borompichaichartkul, C., Srzednicki, G., Panket, W., Piriyaunsakul, S., & Zhao, J. (2012). Microencapsulation of kaffir lime oil and its functional properties. *Drying Technology*, 30(9), 914-920. <https://doi.org/10.1080/07373937.2012.666777>
- Ahmed, A. F., Attia, F. A. K., Liu, Z., Li, C., Wei, J., & Kang, W. (2019). Antioxidant activity and total phenolic content of essential oils and extracts of sweet basil (*Ocimum basilicum* L.) plants. *Food Science and Human Wellness*, 8(3), 299-305. <https://doi.org/10.1016/j.fshw.2019.07.004>
- Ashaari, N. S., Mohamad, N. E., Afzinizam, A. H., Rahim, M. H. A., Lai, K. S., & Abdullah, J. O. (2021). Chemical composition of hexane-extracted plectranthus amboinicus leaf essential oil: Maximizing contents on harvested plant materials. *Applied Sciences*, 11(22), Article 10838. <https://doi.org/10.3390/app112210838>
- Aziz, F. R. A., Jai, J., Raslan, R., & Subuki, I. (2015). Microencapsulation of essential oils application in textile: A review. *Advanced Materials Research*, 1113, 346-351. <https://doi.org/10.4028/www.scientific.net/amr.1113.346>
- Aziz, F. R. A., Jai, J., Raslan, R., & Subuki, I. (2016). Microencapsulation of citronella oil by complex coacervation using chitosan-gelatin (b) system: Operating design, preparation and characterization. *MATEC Web of Conferences*, 69, Article 04002. <https://doi.org/10.1051/mateconf/20166904002>
- Aziz, S., Gill, J., Dutilleul, P., Neufeld, R., & Kermasha, S. (2014). Microencapsulation of krill oil using complex coacervation. *Journal of Microencapsulation*, 31(8), 774-784. <https://doi.org/10.3109/02652048.2014.932028>
- Bakry, A. M., Abbas, S., Ali, B., Majeed, H., Abouelwafa, M. Y., Mousa, A., & Liang, L. (2016). Microencapsulation of oils: A comprehensive review of benefits, techniques, and applications. *Comprehensive Reviews in Food Science and Food Safety*, 15(1), 143-182. <https://doi.org/10.1111/1541-4337.12179>
- Burgess, D. J., & Carless, J. E. (1984). Microelectrophoretic studies of gelatin and acacia for the prediction of complex coacervation. *Journal of Colloid and Interface Science*, 98(1), 1-8. [https://doi.org/10.1016/0021-9797\(84\)90472-7](https://doi.org/10.1016/0021-9797(84)90472-7)
- Burgess, D. J., & Carless, J. E. (1985). Manufacture of gelatin/gelatin coacervate microcapsules. *International Journal of Pharmaceutics*, 27(1), 61-70. [https://doi.org/10.1016/0378-5173\(85\)90185-1](https://doi.org/10.1016/0378-5173(85)90185-1)
- Cheung, R. C. F., Ng, T. B., Wong, J. H., & Chan, W. Y. (2015). Chitosan: An update on potential biomedical and pharmaceutical applications. *Marine Drugs*, 13(8), 5156-5186. <https://doi.org/10.3390/md13085156>
- Comunian, T. A., & Favaro-Trindade, C. S. (2016). Microencapsulation using biopolymers as an alternative to produce food enhanced with phytosterols and omega-3 fatty acids: A review. *Food Hydrocolloids*, 61, 442-457. <https://doi.org/10.1016/j.foodhyd.2016.06.003>
- De Matos, E. F., Scopel, B. S., & Dettmer, A. (2018). Citronella essential oil microencapsulation by complex coacervation with leather waste gelatin and sodium alginate. *Journal of Environmental Chemical Engineering*, 6(2), 1989-1994. <https://doi.org/10.1016/j.jece.2018.03.002>

- Dima, C., Pătrașcu, L., Cantaragiu, A., Alexe, P., & Dima, Ș. (2016). The kinetics of the swelling process and the release mechanisms of *Coriandrum sativum* L. essential oil from chitosan/alginate/inulin microcapsules. *Food Chemistry*, *195*, 39-48. <https://doi.org/10.1016/j.foodchem.2015.05.044>
- Do, Q. D., Angkawijaya, A. E., Tran-Nguyen, P. L., Huynh, L. H., Soetaredjo, F. E., Ismadji, S., & Ju, Y. H. (2014). Effect of extraction solvent on total phenol content, total flavonoid content, and antioxidant activity of *Limnophila aromatica*. *Journal of Food and Drug Analysis*, *22*(3), 296-302. <https://doi.org/10.1016/j.jfda.2013.11.001>
- Dong, Z. J., Touré, A., Jia, C. S., Zhang, X. M., & Xu, S. Y. (2007). Effect of processing parameters on the formation of spherical multinuclear microcapsules encapsulating peppermint oil by coacervation. *Journal of Microencapsulation*, *24*(7), 634-646. <https://doi.org/10.1080/02652040701500632>
- Eghbal, N., & Choudhary, R. (2018). Complex coacervation: Encapsulation and controlled release of active agents in food systems. *LWT*, *90*, 254-264. <https://doi.org/10.1016/j.lwt.2017.12.036>
- Elzoghby, A. O. (2013). Gelatin-based nanoparticles as drug and gene delivery systems: Reviewing three decades of research. *Journal of Controlled Release*, *172*(3), 1075-1091. <https://doi.org/10.1016/j.jconrel.2013.09.019>
- Emamverdian, P., Moghaddas Kia, E., Ghanbarzadeh, B., & Ghasempour, Z. (2020). Characterization and optimization of complex coacervation between soluble fraction of Persian gum and gelatin. *Colloids and Surfaces A: Physicochemical and Engineering Aspects*, *607*, Article 125436. <https://doi.org/10.1016/j.colsurfa.2020.125436>
- Espinosa-Andrews, H., Enríquez-Ramírez, K. E., García-Márquez, E., Ramírez-Santiago, C., Lobato-calleros, C., & Vernon-Carter, J. (2013). Interrelationship between the zeta potential and viscoelastic properties in coacervates complexes. *Carbohydrate Polymers*, *95*(1), 161-166. <https://doi.org/10.1016/j.carbpol.2013.02.053>
- Fan, S., Wang, D., Wen, X., Li, X., Fang, F., Richel, A., Xiao, N., Fauconnier, M., Hou, C., & Zhang, D. (2023). Incorporation of cinnamon essential oil-loaded pickering emulsion for improving antimicrobial properties and control release of chitosan/gelatin films. *Food Hydrocolloids*, *138*, Article 108438. <https://doi.org/10.1016/j.foodhyd.2022.108438>
- Fang, Z., & Bhandari, B. (2010). Encapsulation of polyphenols - A review. *Trends in Food Science and Technology*, *21*(10), 510-523. <https://doi.org/10.1016/j.tifs.2010.08.003>
- Fraj, J., Petrović, L., Đekić, L., Budinčić, J. M., Bučko, S., & Katona, J. (2021). Encapsulation and release of vitamin C in double W/O/W emulsions followed by complex coacervation in gelatin-sodium caseinate system. *Journal of Food Engineering*, *292*, Article 110353. <https://doi.org/10.1016/j.jfoodeng.2020.110353>
- Ghadermazi, R., Asl, A. K., & Tamjidi, F. (2019). Optimization of whey protein isolate-quince seed mucilage complex coacervation. *International Journal of Biological Macromolecules*, *131*, 368-377. <https://doi.org/10.1016/j.ijbiomac.2019.03.026>
- Gharanjig, H., Gharanjig, K., Hosseinezhad, M., & Jafari, S. M. (2020). Development and optimization of complex coacervates based on zedo gum, cress seed gum and gelatin. *International Journal of Biological Macromolecules*, *148*, 31-40. <https://doi.org/10.1016/j.ijbiomac.2020.01.115>

- Girardi, N. S., García, D., Passone, M. A., Nesci, A., & Etcheverry, M. (2017). Microencapsulation of *Lippia turbinata* essential oil and its impact on peanut seed quality preservation. *International Biodeterioration and Biodegradation*, *116*, 227-233. <https://doi.org/10.1016/j.ibiod.2016.11.003>
- Gonçalves, N. D., Grosso, C. R. F., Rabelo, R. S., Hubinger, M. D., & Prata, A. S. (2018). Comparison of microparticles produced with combinations of gelatin, chitosan and gum Arabic. *Carbohydrate Polymers*, *196*, 427-432. <https://doi.org/10.1016/j.carbpol.2018.05.027>
- Houng, P., Ly, K., & Lay, S. (2023). Valorization of kaffir lime peel through extraction of essential oil and process optimization for phenolic compounds. *Journal of Chemical Technology & Biotechnology*, *98*(11), 2745-2753. <https://doi.org/10.1002/jctb.7354>
- Hussein, A. M. S., Lotfy, S. N., Kamil, M. M., & Hassan, M. E. (2016). Effect of microencapsulation on chemical composition and antioxidant activity of cumin and fennel essential oils. *Research Journal of Pharmaceutical, Biological and Chemical Sciences*, *7*(3), 1565-1574.
- Kang, M. K., Dai, J., & Kim, J. C. (2012). Ethylcellulose microparticles containing chitosan and gelatin: pH-dependent release caused by complex coacervation. *Journal of Industrial and Engineering Chemistry*, *18*(1), 355-359. <https://doi.org/10.1016/j.jiec.2011.11.099>
- Kaushik, P., Dowling, K., Barrow, C. J., & Adhikari, B. (2015). Complex coacervation between flaxseed protein isolate and flaxseed gum. *Food Research International*, *72*, 91-97. <https://doi.org/10.1016/j.foodres.2015.03.046>
- Lakkis, J. M. (2016). *Encapsulation and controlled release technologies in food systems*. John Wiley & Sons. <https://doi.org/10.1002/9781118946893>
- Lemetter, C. Y. G., Meeuse, F. M., & Zuidam, N. J. (2009). Control of the morphology and the size of complex coacervate microcapsules during scale-up. *AIChE Journal*, *55*(6), 1487-1496. <https://doi.org/10.1002/aic.11816>
- Lubinska-Szczygeł, M., Różańska, A., Dymerski, T., Namieśnik, J., Katrich, E., & Gorinstein, S. (2018). A novel analytical approach in the assessment of unprocessed kaffir lime peel and pulp as potential raw materials for cosmetic applications. *Industrial Crops and Products*, *120*, 313-321. <https://doi.org/10.1016/j.indcrop.2018.04.036>
- Lv, Y., Zhang, X., Abbas, S., & Karangwa, E. (2012). Simplified optimization for microcapsule preparation by complex coacervation based on the correlation between coacervates and the corresponding microcapsule. *Journal of Food Engineering*, *111*(2), 225-233. <https://doi.org/10.1016/j.jfoodeng.2012.02.030>
- Lv, Y., Zhang, X., Zhang, H., Abbas, S., & Karangwa, E. (2013). The study of pH-dependent complexation between gelatin and gum arabic by morphology evolution and conformational transition. *Food Hydrocolloids*, *30*(1), 323-332. <https://doi.org/10.1016/j.foodhyd.2012.06.007>
- Manaf, M. A., Subuki, I., Jai, J., Raslan, R., & Mustapa, A. N. (2018, May). Encapsulation of volatile citronella essential oil by coacervation: Efficiency and release study. In *IOP Conference Series: Materials Science and Engineering* (Vol. 358, p. 012072). IOP Publishing. <https://doi.org/10.1088/1757-899X/358/1/012072>

- Meka, V. S., Sing, M. K. G., Pichika, M. R., Nali, S. R., Kolapalli, V. R. M., & Kesharwani, P. (2017). A comprehensive review on polyelectrolyte complexes. *Drug Discovery Today*, 22(11), 1697-1706. <https://doi.org/10.1016/j.drudis.2017.06.008>
- Mousavi, M. M., Torbati, M., Farshi, P., Hosseini, H., Mohammadi, M. A., Hosseini, S. M., & Hosseinzadeh, S. (2021). Evaluation of design and fabrication of food-grade nanofibers from chitosan-gelatin for nanoencapsulation of stigmasterol using the electrospinning method. *Advanced Pharmaceutical Bulletin*, 11(3), 514-521. <https://doi.org/10.34172/apb.2021.059>
- Ngamekaue, N., & Chitprasert, P. (2019). Effects of beeswax-carboxymethyl cellulose composite coating on shelf-life stability and intestinal delivery of holy basil essential oil-loaded gelatin microcapsules. *International Journal of Biological Macromolecules*, 135, 1088-1097. <https://doi.org/10.1016/j.ijbiomac.2019.06.002>
- Oliveira, W. Q., Araújo, A. W. O., Wurlitzer, N. J., & Maria, S. R. (2019). Effect of the reaction volume on the formation of microparticles of the pequi (*Caryocar coriaceum* Wittm.) oil by complex coacervation. *Chemical Engineering Transactions*, 74, 445-450. <https://doi.org/10.3303/CET1974075>
- Otálora, M. C., Castaño, J. A. G., & Wilches-Torres, A. (2019). Preparation, study and characterization of complex coacervates formed between gelatin and cactus mucilage extracted from cladodes of *Opuntia ficus-indica*. *LWT*, 112, Article 108234. <https://doi.org/10.1016/j.lwt.2019.06.001>
- Othman, S. N. A. M., Hassan, M. A., Nahar, L., Basar, N., Jamil, S., Sarker, S., Othman, S. M., Hassan, M. A., Nahar, L., Basar, N., Jamil, S., & Sarker, S. (2016). Essential oils from the Malaysian citrus (Rutaceae) medicinal plants. *Medicines*, 3(2), Article 13. <https://doi.org/10.3390/medicines3020013>
- Pedro, A. S., Cabral-Albuquerque, E., Ferreira, D., & Sarmiento, B. (2009). Chitosan: An option for development of essential oil delivery systems for oral cavity care? *Carbohydrate Polymers*, 76(4), 501-508. <https://doi.org/10.1016/j.carbpol.2008.12.016>
- Phong, W. N., Gibberd, M. R., Payne, A. D., Dykes, G. A., & Coorey, R. (2022). Methods used for extraction of plant volatiles have potential to preserve truffle aroma: A review. *Comprehensive Reviews in Food Science and Food Safety*, 21(2), 1677-1701. <https://doi.org/10.1111/1541-4337.12927>
- Poshadri, A., & Aparna, K. (2010). Microencapsulation technology: A review. *Journal of Research ANGRAU*, 38(1), 86-102.
- Prata, A. S., & Grosso, C. R. F. (2015). Production of microparticles with gelatin and chitosan. *Carbohydrate Polymers*, 116, 292-299. <https://doi.org/10.1016/j.carbpol.2014.03.056>
- Qin, X., Lu, Y., Peng, Z., Fan, S., & Yao, Y. (2018). Systematic chemical analysis approach reveals superior antioxidant capacity via the synergistic effect of flavonoid compounds in red vegetative tissues. *Frontiers in Chemistry*, 6, Article 314274. <https://doi.org/10.3389/fchem.2018.00009>
- Raksa, A., Sawaddee, P., Raksa, P., & Aldred, A. K. (2017). Microencapsulation, chemical characterization, and antibacterial activity of Citrus hystrix DC (kaffir lime) peel essential oil. *Monatshefte Fur Chemie*, 148, 1229-1234. <https://doi.org/10.1007/s00706-017-2015-8>

- Rosli, N. A., Hasham, R., & Aziz, A. A. (2018). Design and physicochemical evaluation of nanostructured lipid carrier encapsulated zingiber zerumbet oil by d-optimal mixture design. *Jurnal Teknologi*, 80(3), 105-113. <https://doi.org/10.11113/jt.v80.11268>
- Roy, J. C., Giraud, S., Ferri, A., Mossotti, R., Guan, J., & Salaün, F. (2018). Influence of process parameters on microcapsule formation from chitosan - Type B gelatin complex coacervates. *Carbohydrate Polymers*, 198, 281-293. <https://doi.org/10.1016/j.carbpol.2018.06.087>
- Rungwasantisuk, A., & Raibhu, S. (2020). Application of encapsulating lavender essential oil in gelatin/gum-Arabic complex coacervate and varnish screen-printing in making fragrant gift-wrapping paper. *Progress in Organic Coatings*, 149, Article 105924. <https://doi.org/10.1016/j.porgcoat.2020.105924>
- Shetta, A., Kegere, J., & Mamdouh, W. (2019). Comparative study of encapsulated peppermint and green tea essential oils in chitosan nanoparticles: Encapsulation, thermal stability, in-vitro release, antioxidant and antibacterial activities. *International Journal of Biological Macromolecules*, 126, 731-742. <https://doi.org/10.1016/j.ijbiomac.2018.12.161>
- Shi, L., Beamer, S. K., Yang, H., & Jaczynski, J. (2018). Micro-emulsification/encapsulation of krill oil by complex coacervation with krill protein isolated using isoelectric solubilization/precipitation. *Food Chemistry*, 244, 284-291. <https://doi.org/10.1016/j.foodchem.2017.10.050>
- Shinde, U. A., & Nagarsenker, M. S. (2009). Characterization of gelatin-sodium alginate complex coacervation system. *Indian Journal of Pharmaceutical Sciences*, 71(3), 313-317. <https://doi.org/10.4103/0250-474X.56033>
- Silva, M. C., & Andrade, C. T. (2009). Evaluating conditions for the formation of chitosan/gelatin microparticles. *Polimeros*, 19(2), 133-137. <https://doi.org/10.1590/S0104-14282009000200010>
- Singh, N., & Sheikh, J. (2022). Novel Chitosan-Gelatin microcapsules containing rosemary essential oil for the preparation of bioactive and protective linen. *Industrial Crops and Products*, 178, Article 114549. <https://doi.org/10.1016/j.indcrop.2022.114549>
- Sogias, I. A., Khutoryanskiy, V. V., & Williams, A. C. (2010). Exploring the factors affecting the solubility of chitosan in water. *Macromolecular Chemistry and Physics*, 211(4), 426-433. <https://doi.org/10.1002/macp.200900385>
- Sreepian, A., Sreepian, P. M., Chanthong, C., Mingkhwancheep, T., & Prathit, P. (2019). Antibacterial activity of essential oil extracted from *Citrus hystrix* (kaffir lime) peels: An in vitro study. *Tropical Biomedicine*, 36(2), 531-541.
- Srifuengfung, S., Bunyaphatsara, N., Satitpatipan, V., Tribuddharat, C., Junyaprasert, V. B., Tungrugsasut, W., & Srisukh, V. (2020). Antibacterial oral sprays from kaffir lime (*Citrus hystrix* DC.) fruit peel oil and leaf oil and their activities against respiratory tract pathogens. *Journal of Traditional and Complementary Medicine*, 10(6), 594-598. <https://doi.org/10.1016/j.jtcme.2019.09.003>
- Timilsena, Y. P., Akanbi, T. O., Khalid, N., Adhikari, B., & Barrow, C. J. (2019). Complex coacervation: Principles, mechanisms and applications in microencapsulation. *International Journal of Biological Macromolecules*, 121, 1276-1286. <https://doi.org/10.1016/j.ijbiomac.2018.10.144>

- Timilsena, Y. P., Wang, B., Adhikari, R., & Adhikari, B. (2016). Preparation and characterization of chia seed protein isolate-chia seed gum complex coacervates. *Food Hydrocolloids*, 52, 554-563. <https://doi.org/10.1016/j.foodhyd.2015.07.033>
- Venkatachalam, K. (2019). Changes in phytochemicals and antioxidant properties of kaffir lime leaves under chilling storage. *Kaen Kaset= Khon Kaen Agriculture Journal*, 47(Suppl. 1), 531-536.
- Vishwakarma, G. S., Gautam, N., Babu, J. N., Mittal, S., & Jaitak, V. (2016). Polymeric encapsulates of essential oils and their constituents: A review of preparation techniques, characterization, and sustainable release mechanisms. *Polymer Reviews*, 56(4), 668-701. <https://doi.org/10.1080/15583724.2015.1123725>
- Wang, B., Adhikari, B., & Barrow, C. J. (2014). Optimisation of the microencapsulation of tuna oil in gelatin-sodium hexametaphosphate using complex coacervation. *Food Chemistry*, 158, 358-365. <https://doi.org/10.1016/j.foodchem.2014.02.135>
- Wang, B., Akanbi, T. O., Agyei, D., Holland, B. J., & Barrow, C. J. (2018). Coacervation technique as an encapsulation and delivery tool for hydrophobic biofunctional compounds. In A. M. Grumezescu & A. M. Holban (Eds.), *Role of Materials Science in Food Bioengineering* (pp. 235-261). Academic Press. <https://doi.org/10.1016/C2016-0-00658-7>
- Wang, H., Lin, X., Zhu, J., Yang, Y., Qiao, S., Jiao, B., Ma, L., & Zhang, Y. (2023). Encapsulation of lutein in gelatin type A/B-chitosan systems via tunable chains and bonds from tweens: Thermal stability, rheologic property and food 2D/3D printability. *Food Research International*, 173, Article 113392. <https://doi.org/10.1016/j.foodres.2023.113392>
- Wijaya, Y. A., Widyadinata, D., Irawaty, W., & Ayucitra, A. (2017). Fractionation of phenolic and flavonoid compounds from kaffir lime (*Citrus hystrix*) peel extract and evaluation of antioxidant activity. *Reaktor*, 17(3), 111-117. <https://doi.org/10.14710/reaktor.17.3.111-117>
- Yan, C., & Zhang, W. (2014). Coacervation processes. In R. Sobel (Ed.), *Microencapsulation in the Food Industry: A Practical Implementation Guide* (pp. 125-137). Academic Press. United States. <https://doi.org/10.1016/C2012-0-00852-6>
- Yang, J., Han, S., Zheng, H., Dong, H., & Liu, J. (2015). Preparation and application of micro/nanoparticles based on natural polysaccharides. *Carbohydrate Polymers*, 123, 53-66. <https://doi.org/10.1016/j.carbpol.2015.01.029>
- Yu, F., Li, Z., Zhang, T., Wei, Y., Xue, Y., & Xue, C. (2017). Influence of encapsulation techniques on the structure, physical properties, and thermal stability of fish oil microcapsules by spray drying. *Journal of Food Process Engineering*, 40(6), Article e12576. <https://doi.org/10.1111/jfpe.12576>